# Direct evaluation of phase coexistence by molecular simulation via integration along the saturation line

David A. Kofke
*Department of Chemical Engineering, State University of New York at Buffalo, Buffalo, New York 14260-4200*

(Received 23 October 1992; accepted 4 December 1992)

Thermodynamic integration along a path that coincides with the saturation line is proposed as an efficient means for evaluation of phase equilibria by molecular simulation. The technique allows coexistence to be determined by just one simulation, without ever attempting or performing particle insertions. Prior knowledge of one coexistence point is required to start the procedure. Integration then advances from this state according to the Clapeyron formula—a first-order ordinary differential equation that prescribes how the pressure must change with temperature to maintain coexistence. The method is unusual in the context of thermodynamic integration in that the path is not known at the outset of the process; results from each simulation determine the course that the integration subsequently takes. Predictor–corrector methods among standard numerical techniques are shown to be particularly well suited for this type of integration. A typical integration step along the saturation line proceeds as follows: An increment in the temperature is chosen, and the saturation pressure at the new temperature is "predicted" from previous data (the initial coexistence datum and/or previous simulations). Simultaneous but independent NPT simulations of the coexisting phases are initiated at the said conditions. Averages taken throughout the simulations are repeatedly used to "correct" the estimate of the pressure to convergence. Thus strictly the pressure is not fixed during the simulation. Vapor–liquid coexistence of the van der Waals model is first used to study the numerical integration method without the complications of molecular simulation. In a second application the phase envelope of the Lennard-Jones model fluid is computed, and many variations of the technique are examined. Overall, the results are remarkably consistent and in agreement with previous simulation studies. Difficulty is encountered upon approach of the critical point, but, by artificially coupling the simulation volumes, the method remains effective in this regime so long as a suitably small integration step is employed. Many extensions and improvements of the technique are discussed.

## I. INTRODUCTION

In many circles simulation has come to be regarded as the third leg—along with theory and experiment—upon which we build our understanding of nature. Molecular simulation, comprising molecular dynamics and the Monte Carlo method, is the tool of thermal physics.[1] While nothing approaching macroscopic systems can be simulated with present-day hardware and techniques, molecular simulation methods have proven amazingly successful at enhancing our understanding of matter. The spectrum of properties amenable to analysis by simulation is wide, although the degree of success is not uniform. Not surprisingly, direct molecular simulation functions best when applied to short-wavelength, high-frequency phenomena, and its efficacy diminishes as the relevant length and time scales increase (or, more to the point, as they broaden), culminating in complete failure at the critical point (notwithstanding indirect techniques such as finite-size scaling, which Bruce and Wilding[2] used recently and with great success to study the liquid–gas critical point of the Lennard-Jones fluid in two dimensions). Direct simulation of truly macroscopic systems will not become possible in the foreseeable future, so improvement in technique must be used to overcome the limits of computation.

For decades the direct simulation of phase coexistence was deemed impossible because of the large length scale needed for relaxation of the properties from one phase to the other—attempts to simulate coexisting phases become overwhelmed by the behavior of the interface. The approach that evolved was to evaluate the thermodynamic properties of each phase individually, determine if they satisfied the requirements of mutual thermodynamic equilibrium, and iterate until the point of coexistence was found. The difficulty of this procedure is compounded by the renowned problems inherent in the calculation of the chemical potential.[1] Thermodynamic integration was often used for this determination because the technique is robust, and the path chosen to perform the integration could often be made to coincide with the search for coexistence. Nevertheless, in even the best circumstances, evaluation of the coexistence envelope was a challenging task, and it was not unusual to devote a Ph.D. thesis largely to the computation of the phase diagram of a model substance.

A great advance in simulation technique has reduced this task to a fraction of its original difficulty. The introduction[3] and refinement[4,5] by Panagiotopoulos and coworkers of the Gibbs ensemble simulation technique has made possible the direct evaluation of phase coexistence by

 0021-9606/93/054149-14$06.00  

Monte Carlo simulation. The remarkably simple solution developed by these workers was to remove the interface: The coexisting phases are simulated in separate but thermodynamically coupled volumes, thereby retaining the relevant physics while eliminating the confounding but irrelevant features. The method—now widely accepted—has been applied to many systems and a good, very recent review surveys these developments.[6]

A significant complicating feature of the Gibbs ensemble technique is its reliance on particle exchange to enforce equality of chemical potentials between the coexisting phases. The limitations introduced by this step are substantial, yet remarkable progress is being made in surmounting them.[7,8] Unfortunately there remain many interesting coexistence phenomena that have not and likely will not prove amenable to study with the Gibbs ensemble technique (at least not in its present, appealingly simple implementation). Motivated by these shortcomings, and inspired by the Gibbs ensemble method itself, we recently proposed "Gibbs–Duhem integration" as a complement to the Gibbs ensemble.[9] This method too relies on simultaneous simulation of weakly coupled phases to permit direct evaluation of coexistence, but it does so without reliance on particle exchange. Instead, thermodynamic integration is introduced in a manner that insures chemical potential equality between the phases; a similar idea was exploited by Bruce and Wilding in their study of coexistence and criticality in the two-dimensional Lennard-Jones fluid.[2] In short, the method offers the efficiency of the Gibbs ensemble and the versatility of thermodynamic integration. The purpose of this report is to review and elaborate on the details omitted from our brief communication that introduced the Gibbs–Duhem technique.

The Gibbs–Duhem equation for a pure substance may be written[10]

$$d(\beta\mu) = h\, d\beta + \beta v\, dP, \tag{1.1}$$

where $\mu$ is the chemical potential, $h$ and $v$ are the molar enthalpy and volume, respectively, $P$ is the pressure, and $\beta = 1/kT$, with $k$ the Boltzmann's constant and $T$ the absolute temperature. For two coexisting phases $\alpha$ and $\gamma$ to remain in equilibrium when the temperature is changed, the pressure must vary in a manner that maintains chemical potential equality between them. The required change is easily derived from Eq. (1.1),[10] and is given by the Clapeyron equation

$$\left(\frac{dP}{d\beta}\right)_\sigma = -\frac{\Delta h}{\beta \Delta v}, \tag{1.2}$$

where $\Delta h = h_\alpha - h_\gamma$ is the difference in molar enthalpies of the coexisting phases, and $\Delta v$ is defined similarly as $v_\alpha - v_\gamma$; the subscript $\sigma$ indicates that the derivative is taken along the saturation line. Viewed mathematically, Eq. (1.2) is simply a first-order nonlinear differential equation which—given an "initial condition"—yields upon integration the vapor-pressure curve. Many techniques are available for the numerical treatment of these equations,[11–14] and, in principle, there is no reason that they cannot be applied here. The complication of course is in the nature of the right-hand side of the formula—for model substances it can be accurately evaluated only by molecular simulation. This procedure is very expensive by the standards of typical numerical analysis, so many of the usual techniques are entirely inappropriate here. Nevertheless, it is not difficult to take some integration techniques "off the shelf" and to modify them slightly to take advantage of the unique nature of "function evaluations" by molecular simulation. The result is a method that allows direct determination of the coexistence envelope through a series of simulations. Each simulation yields one point of the coexistence line, and most importantly it does so without the need to perform particle insertions.

The method outlined above is straightforward, but there are several ways in which it may be implemented. We discuss these issues and present our approach in the next section. We then demonstrate the technique by computing the vapor–liquid coexistence envelope for the van der Waals and the Lennard-Jones model fluids. In the final section we discuss in some detail how the method may be extended to more interesting systems—including mixtures—and we review some of the limitations of the technique that may be encountered when applied in these and other situations.

## II. METHOD

### A. Integrator

The difficulty found in the numerical integration of differential equations—as opposed to numerical quadrature—is that the integrand [the right-hand side of Eq. (1.2), call it $f$] depends on both the independent and dependent variables [let us denote them $x$ and $y$, respectively, so that $y=y(x)$ and $f=f(x,y)$]. At the outset of each integration step (in which $x_n$ is incremented to $x_{n+1}$) the value of $y_{n+1}=y(x_{n+1})$ is unknown; moreover, accurate evaluation of it requires knowledge of $f_{n+1} = f(x_{n+1},y_{n+1})$. Consequently, the integration procedure is inherently an iterative process. The most accurate and stable integration algorithms[11–14] typically require several integrand evaluations to advance one step in the independent variable. The first of these gives a feel for the behavior of $f(x,y)$ in the uncharted region, and this information is used—sometimes in combination with knowledge of the prior behavior of $y(x)$ and $f(x,y)$—to provide a best estimate for $y_{n+1}$; the process then repeats for the next increment in $x$. Those algorithms that are generally acknowledged as the best require evaluation of $f(x,y)$ for several values of $x$ between $x_n$ and $x_{n+1}$. Clearly this is to be avoided in the current application, where each integrand evaluation entails a complete simulation.

Each simulation must yield a coexistence datum if the proposed technique is to be considered a means for direct evaluation of coexistence. Fortunately, the right-hand side of Eq. (1.2) is a smooth function of pressure and temperature, and simple integration schemes can be applied with accurate results. This happy situation likely holds for most other types of coexistence, although it may require the proper formulation of the governing differential equation.

As a simple example, it is well known that when Eq. (1.2) is written

$$\left(\frac{d\ln P}{d\beta}\right)_\sigma = -\frac{\Delta h}{\beta P \Delta v} \tag{2.1}$$

and applied to vapor–liquid equilibrium, the right-hand side is virtually constant. Such an assumption leads to the Clausius–Clapeyron equation, which prescribes a linear relation between $\ln P$ and $1/T$. Although this assumption is not introduced into the numerical technique, any integration scheme that is applied here would benefit from the slowly varying nature of the integrand of Eq. (2.1) as compared to Eq. (1.2).

The nature of integrand evaluations by molecular simulation is quite different from the way one normally thinks about the evaluation of functions, and standard numerical methods for the treatment of differential equations have of course not been designed with simulations in mind. Normally a function is computed by a well-defined sequence of calculations, and the answer is not available until the calculation is complete. Simulation on the other hand is a long process in which the estimate of the quantity of interest is gradually refined until a (somewhat arbitrary) point is reached and the "answer" is given. For an integrator to exploit this feature of simulation, it cannot rely on integrand evaluations at intermediate values of the temperature (which is represented by the independent variable $x$ above). However, once a step in the temperature is taken and simulation is initiated, one need not wait for completion of the run before refining the estimate of the pressure (i.e., the dependent variable $y$). Instead it may be updated in accordance with the best current estimate of $-\Delta h/\beta\Delta v$ (the integrand $f$) as the simulation progresses. Because $f$ depends on averages from both of the coexisting phases, they must be simulated simultaneously to implement this procedure.

All of the considerations discussed above suggest predictor–corrector techniques as the most appropriate choice of integrator.[11–14] In the predictor step, values of $y(x)$ and $f(x,y)$ for a set of (usually equally spaced) values of $x$ ($x_n$, $x_{n-1}$, etc.) are used to construct a polynomial approximation to the functions. These data are obtained from the initial condition and/or from prior simulations. Predictor–corrector techniques differ in how much of and in what manner this information is used; one important parameter is the order of the polynomial, which defines the order of the predictor–corrector method. The polynomial is extrapolated to predict $y(x)$ at $x_{n+1}$; this value we label $y^{(0)}_{n+1}$, where the 0 superscript indicates that it is a predicted value. In the corrector step $f(x_{n+1},y^{(0)}_{n+1})$ is evaluated and the result is used to improve the polynomial fit of $y(x)$, and a corrected value $y^{(1)}_{n+1}$ is generated. The procedure may be repeated to generate $y^{(2)}_{n+1}$, $y^{(3)}_{n+1}$, etc., until convergence, although the accepted wisdom[14] is to halt the process at this point, and to continue with the next step of the integration. However, in the present context this is not the best strategy because the corrector may be easily iterated to convergence during the course of simulation averaging. It should be remembered that the accuracy of the calculation will nevertheless be limited by the polynomial approximation to $y(x)$, and that "iteration to convergence" does not necessarily imply that the error introduced by the integration procedure is negligible.[14]

Startup of a predictor–corrector series is sometimes problematic. Most algorithms require data for several values of $x$, but at the outset only one datum is available (the initial condition). Often other methods are called in to start the procedure. We have avoided this approach, and instead have relied on lower-order predictor–corrector formulas to initiate the procedure. This simple solution may not work in all instances, but it proved successful in our studies. The formulas that we have employed are listed in Table I.[12,13] As seen in the table, the trapezoid method requires only one prior $y(x)$ and $f(x,y)$ value (usually given by the initial condition) for both the predictor and the corrector; the midpoint formula requires two for each, while the Adams predictor and corrector require four and three prior values, respectively. These formulas require that the $x$ values of the series of simulations be equally spaced, with step size $h$. Given the values of $y$ and $f$ for a sequence of states $x_n$, $x_{n-1}$, etc., the formulas indicate how $y_{n+1}$ is to be estimated (predictor) and subsequently updated (corrector) during the simulation once an approximation for $f_{n+1}$ becomes available. Further details are provided below.

### B. Stability

The question of stability of the technique is an important one, and it has several facets. One may first consider propagation of errors as the integration proceeds. If numerical errors from initial integration steps result in even larger errors at subsequent steps, the method is unstable and will not produce reliable results. The stability analysis of numerical techniques is well developed and documented[12,13] and for the most part it will not be repeated here. When choosing an integration scheme often a tradeoff is required between accuracy and stability. The trapezoid corrector for example is not especially accurate but it is locally stable for all step sizes $h$ of the independent variable $x$. Higher-order predictor–corrector methods lose stability as $h$ increases beyond a certain value. It suffices here to say that a principal indicator of stability is the derivative $\partial f/\partial y$; the step size $h$ should be chosen so that the product of it with this derivative is a small quantity.[12]

A second issue of stability has to do with the convergence properties of the corrector iterations.[13] This is essentially a method of successive substitution, and it will converge if

$$ch\left|\frac{\partial f}{\partial y}\right| < 1, \tag{2.2}$$

where $c$ is a constant that is easily determined for a given corrector formula (e.g., $c=1/2$ for the trapezoid formula). The product is the same as that discussed just above. Provided the derivative is finite, this relation can always be satisfied by choosing a sufficiently small step $h$. In practice, the convergence criterion will be less restrictive than this.

Since running averages (as opposed to instantaneous values or recent block averages, see below) of $f(x,y)$ are used to update $y$, the iterations will be considerably damped and thereby enhance the stability of the procedure. Regardless, this consideration highlights the importance of the product $h|\partial f/\partial y|$ to the stability of the numerical calculation.

The final issue of stability is thermodynamic in nature. NPT simulations of coexisting, single-component phases are possible—in apparent violation of the phase rule—only because the pressure is not truly an independent variable. At the outset of each simulation, the first guess for the correct equilibrium pressure contains some error that should diminish as the run progresses. The unavoidable result is that for part of the simulation one of the phases is unstable with respect to the other;[15] there then is the possibility that it may condense or vaporize before the pressure converges to the correct value, and thereby invalidate the results. This event is least likely at low temperatures, where there exist significant regions of metastability for each phase and the free energy barrier between them is large. But upon approach of a critical point the barrier decreases and a catastrophic phase change becomes possible—indeed it is likely—even when the pressure is the correct value for coexistence.

Borrowing again from the Gibbs ensemble[6] method, this potentially serious problem can be alleviated by artificially coupling the volume changes of the two phases. For example, it is simple to perform simultaneous volume changes in a manner that mimics the exchange of particles and volume between the phases. Coupling of the volumes this way prevents either phase from unilaterally vaporizing or condensing. Details are provided in the following section.

### C. Coupling

Let us first write the partition function $\Delta$ for the composite system, assuming that the pressure has converged to the correct coexistence value

$$\Delta(T,P,N_1,N_2)=\delta(T,P,N_1)\delta(T,P,N_2)$$
$$=\int_0^\infty dV_1\int_0^\infty dV_2\exp[-\beta P(V_1+V_2)]$$
$$\times q(T,V_1,N_1)q(T,V_2,N_2), \tag{2.3}$$

where $q(T,V,N)$ and $\delta(T,p,N)$ are the canonical and isothermal–isobaric ensemble partition functions,[16] respectively, for each subsystem. As written in Eq. (2.3), the partition function prescribes a simulation procedure in which the two volumes are sampled independently. Nevertheless, two new variables, each depending on both $V_1$ and $V_2$, may instead be sampled because the Gibbs–Duhem integration procedure requires that simulations of each phase be conducted simultaneously. For vapor–liquid coexistence appropriate choices are suggested by the Gibbs ensemble as formulated by Smit *et al.*: $X$ and $Y$ are defined such that the densities of each phase are[5,17]

$$\rho_1=\frac{X}{Y}\rho,\quad \rho_2=\frac{1-X}{1-Y}\rho, \tag{2.4}$$

where $\rho$ is a density that lies between the expected coexistence densities, but is otherwise arbitrary. As $\rho_j=N_j/V_j$, with $N_1$ and $N_2$ constant throughout the simulation, sampling of $X$ and $Y$ varies the volumes of the two phases. With the stipulation that $X$ and $Y$ be bounded by zero and unity, the densities given by Eq. (2.4) must lie on opposite sides of $\rho$. Thus the desired restriction on the system densities is achieved. To ensure that $X$ and $Y$ do not sample values outside their bounds, it is convenient to define unbounded variables $t_X$ and $t_Y$ such that

$$X=\frac{1}{1+\exp(-t_X)},\quad Y=\frac{1}{1+\exp(-t_Y)}. \tag{2.5}$$

These are the variables that are sampled during the simulation. With them, the partition function takes the form

$$\Delta(T,P,N_1,N_2;\rho)$$
$$=\int_{-\infty}^\infty dt_X\int_{-\infty}^\infty dt_Y J(t_X,t_Y)\exp\{-\beta P[V_1(t_X,t_Y)$$
$$+V_2(t_X,t_Y)]\}q[T,V_1(t_X,t_Y),N_1]$$
$$\times q[T,V_2(t_X,t_Y),N_2], \tag{2.6}$$

where the Jacobian of the transformation $J(t_X,t_Y)$ is

$$J=N_1N_2\frac{(\rho-\rho_1)(\rho_2-\rho)}{\rho\rho_1\rho_2(\rho_1-\rho_2)}. \tag{2.7}$$

### D. Procedure

A Gibbs–Duhem simulation may be performed using Monte Carlo (MC) or molecular dynamics simulation (MD). In the simplest case—employing no artificial coupling of the type just described—two NPT simulations are performed simultaneously. The procedure for conducting NPT MC and MD may be found in many places,[1] and will not be repeated here; it suffices to say that each algorithm requires the input of the pressure as an independent parameter. At the outset the pressure is specified by the predictor formula, and its value governs the conduct of the MC or MD simulations in each box during the initial stages of the run. For example, application of the trapezoid-rule predictor given in Table I to Eq. (2.1) yields

$$P=P_0\exp[f_0h], \tag{2.8}$$

where $f_0$ is by the right-hand side of Eq. (2.1), $P_0$ is the pressure, and both are evaluated from the "initial condition"—data that must be obtained by some other means, possibly a Gibbs ensemble simulation, an accurate theory, or from a thermodynamic integration series performed separately; $h$ is the difference in reciprocal temperature $\beta$ between the current simulation and the initial condition.

Averages of the energy and volume of each phase are collected for a short period, and are then used to update

TABLE I. Predictor–corrector formulas.[12,13] Names are for reference by text. P,C indicate predictor and corrector, respectively. Each formula describes how the pressure (designated here as $y$) in a given simulation (subscripted $i+1$) is determined from $y$ and $f$ (the integrand) of previous simulations (subscripted $i,i-1$, etc.), corresponding to reciprocal temperatures $\beta$ that differ by $h$. For example, if $h=0.05$ and the current simulation ($i+1$) is conducted at $\beta=1.20$, then $y_i$ and $f_i$ are $\ln(P)$ and $f(\beta,P)$ for $\beta=1.15$; $y_{i-1}$ and $f_{i-1}$ are for $\beta=1.10$, etc. $n$ indicates the number of previous simulation state points needed to use each formula.

| Name | Type | $n$ | Formula |
|---|---|---|---|
| Trapezoid | P | 1 | $y_{i+1}=y_i+hf_i$ |
| | C | 1 | $y_{i+1}=y_i+\frac{h}{2}(f_{i+1}+f_i)$ |
| Midpoint | P | 2 | $y_{i+1}=y_{i-1}+2hf_i$ |
| | C | 2 | $y_{i+1}=y_{i-1}+\frac{h}{3}(f_{i+1}+4f_i+f_{i-1})$ |
| Adams | P | 4 | $y_{i+1}=y_i+\frac{h}{24}(55f_i-59f_{i-1}+37f_{i-2}-9f_{i-3})$ |
| | C | 3 | $y_{i+1}=y_i+\frac{h}{24}(9f_{i+1}+19f_i-5f_{i-1}+f_{i-2})$ |

the pressure according to the corrector formula. Again using the trapezoid rule for an example, the pressure is given by

$$P=P_0\exp[h(f_0+f_1)/2], \tag{2.9}$$

where $f_1$ is the estimate of $f$ obtained from the simulation in progress. The simulation continues with the new pressure, and the process repeats after another interval of sampling. Of course $f_0$ never changes during a single simulation, while subsequent values of $f_1$ are best determined from the running averages of the enthalpy and the volume. An alternative would compute $f_1$ from block averages over a limited number of configurations immediately preceding the pressure adjustment step. This choice and others like it have certain drawbacks. Use of the running average causes fluctuations in the pressure to become increasingly damped as the simulation proceeds; absent this effect, block averaging methods would likely be more slowly converging at best, and unstable at worst. More important, use of the running average leads to a final pressure that is consistent with the simulation averages of the energies and volumes of the phases. Any other approach could well result in the uncomfortable circumstance in which the collective simulation data do not obey the Gibbs–Duhem equation—the formula that governs the whole procedure!

With this discussion it should be emphasized that the pressure is in principle not a quantity to be stochastically sampled during a simulation. The Gibbs–Duhem simulation method is a marriage of several numerical techniques, and nominally it is the nature of the pressure evaluation to converge in an analytical sense, and not in a statistical one. Of course the splicing of the techniques makes this separation difficult in practice, but nonetheless it is worthwhile to appreciate the distinction. In a similar vein, we have carefully avoided the term "Gibbs–Duhem ensemble" because there is no well-defined ensemble that is sampled by the simulations. The pressure is not fixed, and an analysis of its "fluctuations" should not proceed as if this were a standard statistical mechanical ensemble.[16]

Introduction of the coupling described above is quite simple when MC sampling is used. Instead of sampling the volumes of each box, random and uniformly distributed steps are taken in $t_X$ and/or $t_Y$. Given the proposed $t_X$ and $t_Y$, the new volumes are easily computed and used as always in deciding acceptance. The Hamiltonian must be modified by the addition of the term $-kT\ln J(t_X,t_Y)$, where $J$ is the Jacobian of Eq. (2.7), and the acceptance criteria adjusted accordingly. Application of the coupling with MD is less clear, although it can likely be achieved by treating $t_X$ and $t_Y$ (or maybe $X$ and $Y$ themselves) as auxiliary dynamical variables, much as is done with the volume in NPT MD.[1] At present we have not pursued this idea further.

## III. APPLICATION

There are many variables to consider in planning a Gibbs–Duhem series. Of particular significance are the following.

*Integration step size.* There is a trade-off between the range of coexistence states that may be investigated by a fixed number of simulations and the stability and accuracy of the predictor–corrector integration.

*The integrand.* Clearly it is best to formulate the governing differential equation with a slowly varying integrand [e.g., Eq. (2.1) vs Eq. (1.2)], but often this is not possible. How sensitive is the technique to this choice?

*The predictor–corrector formula.* A higher-order form is more accurate but requires more input data and may be less stable.

*Coupled vs independent volume changes.* Do the results depend on this choice, and can coupling attenuate the problems expected upon approach of the critical point?

*System size.* An important consideration in any molecular simulation study.

Some of these questions can be addressed before turning to simulation. Indeed, it is worthwhile to study how well predictor–corrector methods can integrate along the saturation line absent the complications introduced by statistical errors. Any thermodynamic model may be used to examine this issue; that of van der Waals is a convenient and well-studied choice.

### A. van der Waals fluid

The van der Waals equation of state may be written

$$P_r=\frac{8}{\beta_r(3v_r-1)}-\frac{3}{v_r^2} \tag{3.1}$$

where $\beta_r$, $v_r$, and $P_r$, respectively, refer to the reciprocal temperature, the molar volume and the pressure divided by their values at the critical point. We performed in various ways Gibbs–Duhem integration from $\beta_r=2$ to very close to the critical ($\beta_r=1$), and examined the error in the saturation pressure at each temperature (the correct pressure may of course be calculated directly by equating temperature, pressure, and chemical potential of the coexisting phases). The predictor–corrector formulas listed in Table I were used, and the corrector was iterated to convergence at each step (specifically, until the ratio of consecutive corrector pressures was within $10^{-5}$ of unity). Startup of each integrator was achieved by computing the required quan-

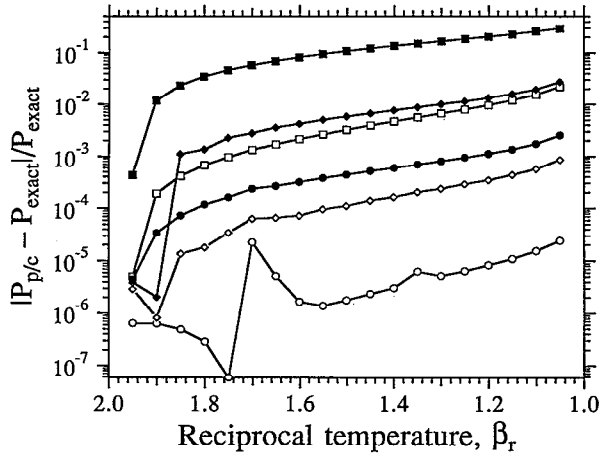


FIG. 1. Fractional error in saturation pressure as a function of reduced reciprocal temperature $\beta_r$ during Gibbs–Duhem integration using the van der Waals equation of state. Integration begins at the left of the figure (low temperature) and proceeds to the right. Filled and open markers describe integration according to Eqs. (1.2) and (2.1), respectively. The shape of the marker indicates the predictor–corrector method: Squares represent the trapezoid formulas; diamonds are the midpoint formulas; circles indicate the Adams formulas.

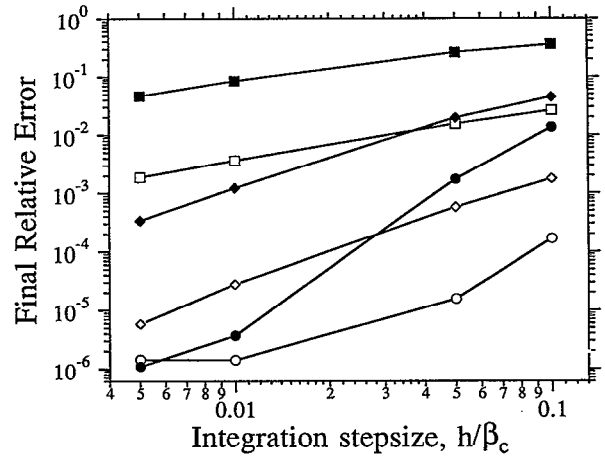


FIG. 2. Effect of integration step size on accuracy of integration according to the van der Waals equation of state. The ordinate is the fractional error in the saturation pressure observed after Gibbs–Duhem integration to a reciprocal temperature $\beta_r=1.1$ from $\beta_r=2.0$. Designation of markers is as in Fig. 1.

tities for $\beta_r>2$ exactly. Special attention was paid to the effect of the governing differential equation [Eq. (1.2) and (2.1)] on the outcome of the integration. In nearly all instances the pressure was determined very accurately, and differences can be uncovered only by looking at the errors on a logarithmic scale.

The influence of the integrator is displayed in Fig. 1. The observed error is consistent with the order of each method: The trapezoid-rule predictor–corrector yields the poorest results and the Adams formulas the best, with the midpoint predictor–corrector in between. With all integrators the error accrues gradually throughout the integration. All methods *under*estimate the correct pressure [this trend cannot be determined from the figure because absolute values are taken to make the logarithmic plot; also the initial erratic behavior of the Adams integration of Eq. (2.1) is an artifact of the plot—the error is actually changing sign at this point]. The governing differential equation has a significant influence. There is a one-to-two orders of magnitude deterioration in the results when Eq. (1.2) rather than Eq. (2.1) is integrated. The trapezoid rule in the former yields an unacceptable result, with an error of more than 20% seen by the end of the integration. In all other applications the results may be deemed acceptable, with an error of a few percent arising in the worst cases. Interestingly, no pathological behavior seems to be surfacing as the critical point is approached, but then again with this step size the approach is not even to within 5% of the critical temperature.

The effect of integration step size is seen in Fig. 2. In this plot the error in the pressure at $\beta_r=1.1$—a temperature near the end of the integration series—is given as a function of the integration step size. As expected, the integration becomes more accurate as the stepsize is decreased (note that a relative error of much less than $10^{-5}$ is not to be expected as this was used to define convergence of the corrector). The improvement is greater for the higher-order integration methods, and this is consistent with the definition of the "order" of a method. The maximum step size that insures convergence of the corrector iterations can be determined directly from Eq. (2.2). In Fig. 3 this general stability indicator is presented as a function of temperature for each formulation of the governing differential equation; a larger value indicates a more stable integration. Two features are apparent. First, a larger step size may be used to integrate Eq. (2.1), indicating that integration of the slowly varying integrand enjoys greater

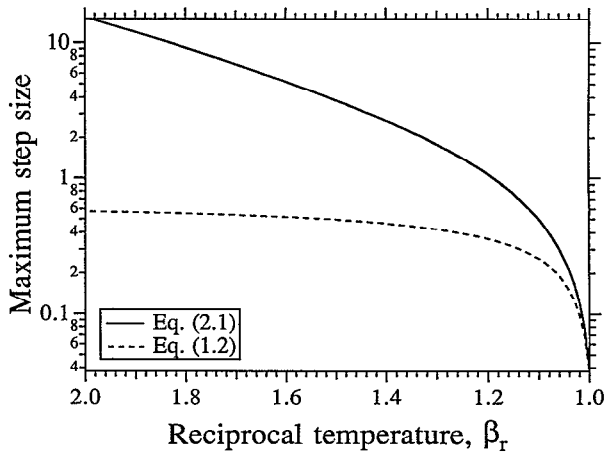


FIG. 3. Theoretical maximum step size $h$ that insures convergence of trapezoid corrector, plotted as a function of reciprocal temperature. Values are computed according to the van der Waals equation of state. The lower line applies for integration according to Eq. (1.2), and the upper line is for Eq. (2.1). The quantity plotted is $2/|\partial f/\partial y|$ [cf. Eq. (2.2)], where $f$ and $y$ are the integrand and the dependent variable [$P$ or $\ln P$ for Eq. (1.2) and (2.1), respectively], as described in the text. Ordinate and abscissa are made dimensionless with $\beta_c$, the reciprocal temperature at the critical point.

TABLE II. Parameters for Gibbs–Duhem series of the Lennard-Jones fluid. "Series" column labels each series for reference in text and figures; the initial condition for each series is also indicated in this column (GE denotes Gibbs-ensemble data of Ref. 4; a letter designates a simulation from the corresponding series). "Initial, final $\beta$" indicates the starting and ending reciprocal temperatures of each series, for which integration steps of "step size" (column 3) were used to integrate "govg Eq." (column 5). "$N$" lists the number of particles used to simulate the liquid and vapor, respectively. "P/C technique" indicates the predictor–corrector scheme used to perform the integration: T—trapezoid rule; $M$—midpoint rule; A—Adams; TMA indicates that the methods were used in succession to achieve startup as described in the text. "Cplng" denotes whether the artificial coupling of Sec. II C was employed. The incidence of "unilateral phase change" is noted, with reference to the phase that underwent the change and at what reciprocal temperature it occurred during the series. Boldface entries highlight variations from the appropriate "base series."

| Series (init'l cond) | Initial, final $\beta$ | Step size, $h$ | $N$, liq/vap | Govg Eq. | P/C Technique | Cplng? | Unilateral phase change? | Notes |
|---|---|---|---|---|---|---|---|---|
| a(GE) | 1.00; 0.80 | 0.05 | 108/108 | (2.1) | TMA | Yes | No | **Base series** |
| b(GE) | 1.00; 1.35 | 0.05 | 108/108 | (2.1) | TMA | Yes | No | **Base series** |
| c(GE) | 1.00; 0.80 | 0.05 | **500/256** | (2.1) | TMA | Yes | No | |
| d(c) | 0.79; 0.76 | 0.01 | 500/256 | (2.1) | TMA | Yes | No | Continues (c) |
| e(GE) | 1.00; 1.35 | 0.05 | 108/108 | (2.1) | TMA | **No** | No | |
| f(GE) | 1.00; 0.80 | 0.05 | 108/108 | (2.1) | TMA | **No** | liq; $\beta$=0.80 | |
| g(f) | 0.83; 0.77 | 0.02 | 108/108 | (2.1) | TMA | No | both; $\beta$=0.77 | Continues (f) |
| h(e) | 1.30; 0.80 | 0.05 | 108/108 | (2.1) | TMA | No | liq; $\beta$=0.80 | **Base series** |
| i (GE) | 1.28; 0.78 | 0.05 | 108/108 | (2.1) | TMA | No | liq; $\beta$=0.78 | |
| j(e) | 1.30; 0.80 | 0.05 | 108/108 | (2.1) | TMA | **Yes** | No | |
| k(j) | 0.79; 0.76 | 0.01 | 108/108 | (2.1) | TMA | Yes | No | Continues (j) |
| l(e) | 1.30; 0.80 | 0.05 | 108/108 | **(1.2)** | TMA | No | No | |
| m(e) | 1.30; 0.80 | 0.05 | 108/108 | (2.1) | **T** | No | liq; $\beta$=0.80 | |
| n(e) | 1.25; 0.85 | **0.10** | 108/108 | (2.1) | TMA | No | No | |
| o(e) | 1.30; 0.80 | 0.05 | **256/256** | (2.1) | TMA | No | No | |
| p(o) | 0.79; 0.76 | 0.01 | 256/256 | (2.1) | TMA | No | liq; $\beta$=0.78 | Continues (o) |
| q(e) | 1.25; 0.85 | **0.10** | 108/108 | **(1.2)** | **T** | No | vap; $\beta$=0.85 | "Worst case" |
| r(h) | 0.84; 0.76 | **0.01** | 108/108 | (2.1) | TMA | Yes | No | |
| s(r) | 0.80; 0.76 | **0.01** | 108/108 | (2.1) | TMA | Yes | No | 30 000 cycle runs |
| t(r) | 0.80; 0.76 | **0.01** | **256/256** | (2.1) | TMA | Yes | No | |

stability as well as improved accuracy. Second, the maximum allowable step size decreases dramatically upon approach of the critical point. This phenomenon does not seem to have caused trouble in any of the numerical studies of this section; nevertheless, it points to the need to take special care when applying Gibbs–Duhem integration near a critical point.

### B. Lennard-Jones fluid

Vapor–liquid coexistence of the Lennard-Jones fluid can be used to study the strengths and limitations of the proposed technique in a more realistic situation. The Lennard-Jones potential is the prototypical model for simple fluids, and its properties are well documented; indeed, the very first test of Gibbs ensemble simulation was performed using the Lennard-Jones potential.[3] In the following, all quantities are made dimensionless with the Lennard-Jones size and energy parameters $\sigma$ and $\epsilon$.

We performed many Gibbs–Duhem integration series investigating the effect of the parameters listed above. Conditions for each series are summarized in Table II, where a letter label is assigned to each. The series may be grouped into two categories: in series (a)–(g) the $\beta$=1.0 Gibbs-ensemble data of Panagiotopoulos *et al.*[4] served as the initial condition and integration was performed in each direction, approaching the triple and critical points, respectively; series (h)–(t) used the $\beta$=1.35 data from the termination of series (e) as the initial condition, and integration was performed toward the critical point. This starting condition was preferred because it would allow errors more chance to accumulate and thus better test the limits of the technique. One additional run—series (i)—was performed using $\beta$=1.33 Gibbs-ensemble data[4] as the initial condition, but this gave unacceptable results. For each grouping one "base series" was chosen. The effect of each operating parameter was explored by conducting series that varied from this base case by only one parameter. These parameters are highlighted in Table II. The last three series—(r), (s), and (t)—focus on the approach to the critical point. The coupling method of Sec. II C was introduced to eliminate unilateral phase transitions in some series as noted in the table. For each simulation the arbitrary "overall density" $\rho$ needed to implement the method was chosen by averaging the liquid and vapor densities of the preceding run of the series.

Each simulation was conducted in the manner described in Sec. III D. The simulations were organized in cycles, where each cycle comprised on average one attempted displacement per particle and two attempted volume changes (the type of move was selected randomly); the sizes of all attempted changes were adjusted to achieve a 50% acceptance rate. All simulations sampled 10 000 cycles beyond an equilibration period that usually lasted 1000 cycles (the exceptions being the few simulations that started from an fcc lattice configuration, in which equilibration lasted 10 000 cycles, and series (s), in which each

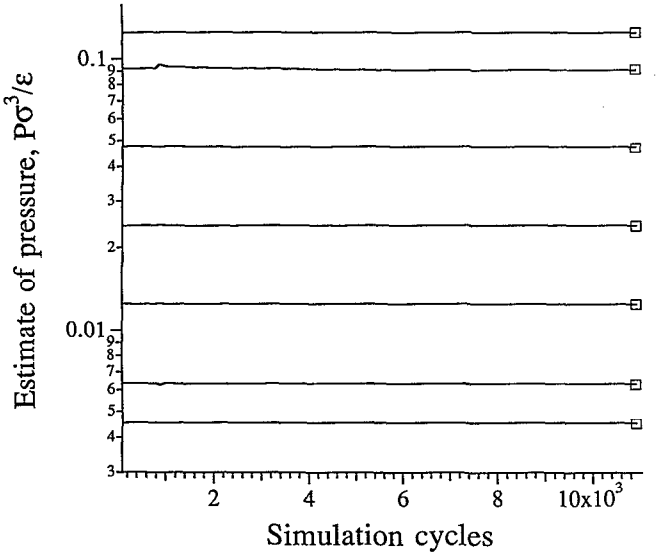


FIG. 4. The pressure as estimated by the corrector during the course of several series (o) simulations. The glitch at 1000 cycles results from discarding of the equilibration measurements and accompanying renewal of the running averages of volume and enthalpy. The box at the right is centered on the pressure given by the predictor formula at the outset of the simulation. From bottom to top the reciprocal temperatures $\beta$ are: 1.25, 1.20, 1.10, 1.00, 0.90, 0.80, 0.76 [the last a series (t) simulation].

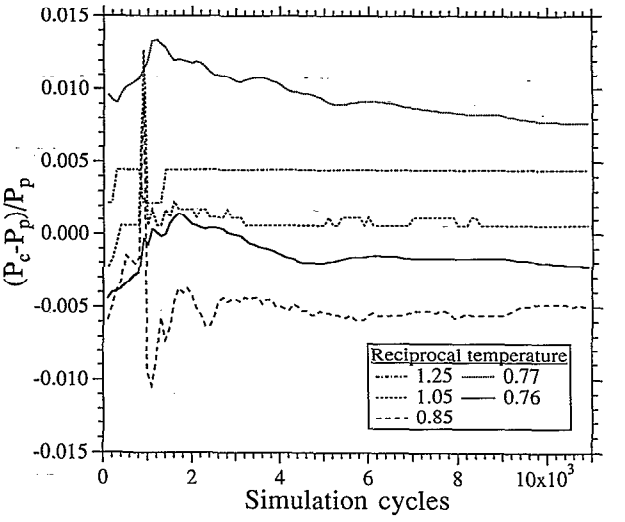


FIG. 5. The pressure as estimated by the corrector ($P_c$) during the course of several simulations from series (o) and (t), given as the fractional deviation from the predictor value ($P_p$). The large fluctuation at 1000 cycles results from discarding of the equilibration measurements. The discrete nature of some of the low-temperature fluctuations is an artifact of the way the plot was generated (the simulation log files recorded the pressure to five decimal places, which is only three significant figures at the lower temperatures).

run sampled 30 000 cycles beyond equilibration). The initial particle placements for each simulation were given by the final configuration of the preceding run. The pressure was adjusted every 10 cycles as described in Sec. II D and further detailed below. All running averages (in particular those used to adjust the pressure) were re-zeroed after the equilibration period. In most simulations 108 particles modeled each phase, and exceptions are noted in the table. Standard periodic boundary conditions were used, the potential was truncated at half the edge length of the (cubic) simulation volume, and the minimum image convention was employed. Appropriate steps were taken to account for changes in the long-range correction to the potential when deciding acceptance of volume changes.[1] Instantaneous values of the internal energy, pressure, and density of each phase were written to disk after every 100 cycles and were subsequently analyzed to estimate the statistical error of the averages.[18]

In almost all the series, integration proceeded with the Adams predictor–corrector.[12,13] As noted above and in Table I, this algorithm requires four prior simulations. Start-up was performed as follows: The first simulation relied on the trapezoid rule predictor–corrector (with the initial-condition data) to determine the pressure; the midpoint formulas were used for the second simulation of a series; in the third the midpoint predictor was used with the Adams corrector; all subsequent simulations of a given series used the Adams formulas. To gauge the sensitivity of the technique on the predictor–corrector algorithm, two series [(m) and (q)] were performed using only the trapezoid-rule formulas. Convergence of the pressure is demonstrated in Figs. 4 and 5. Figure 4 displays the pressure computed by the corrector throughout the course of several series (o) and one series (t) simulation; the predictor pressure is presented for easy comparison with the final pressure of each run. The predictor does a good job of providing an initial estimate, and little fluctuation is seen in the pressure throughout the course of each simulation, even at near-critical temperatures. An expansion of scale is achieved in Fig. 5 by plotting the relative deviation of the corrector pressure from the predictor value through the course of each simulation. The deviation is rarely above 1%, and fluctuations are on the order of just 0.2%, even near the critical point ($\beta$=0.76, approximately)

Figure 6 examines the behavior of the density of each phase as the simulations progress. Given the stability of the pressure displayed in the previous figures, no unusual behavior is expected here nor is it observed. The artificial coupling introduced to preclude unilateral phase transitions substantially influences the sampling. A cursory look at the figure reveals a strong correlation between the liquid and vapor densities at the highest temperature; indeed, the coefficient of correlation is very large, −0.54. This, however, is not a representative value—the coupled simulations typically had coefficients of about −0.3. Further, the midrange profile in the figure is also from a coupled simulation, and the coefficient there is an unusually small 0.008, while the low-temperature simulation employed uncoupled volume sampling and shows a coefficient of 0.04 (a typical value for this type of volume sampling). It is interesting to note that in no simulations did the volumes exchange their roles as liquid and vapor, even when very near the critical point. Such exchanges are not unusual during a Gibbs ensemble simulation, and they are not precluded by the coupling algorithm of a Gibbs–Duhem simulation.

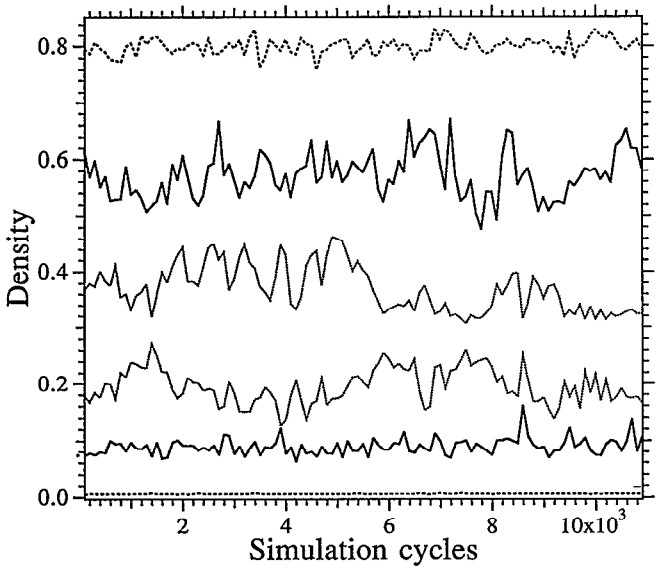


FIG. 6. Densities of the coexisting phases through the course of several simulations. The dashed-line, outermost profiles (note that one is very close to zero) represent the series (o) $\beta=1.25$ run; the solid lines are from the series (r) $\beta=0.84$ simulation, and the dotted-line, innermost pair describe the series (t) $\beta=0.76$ run.

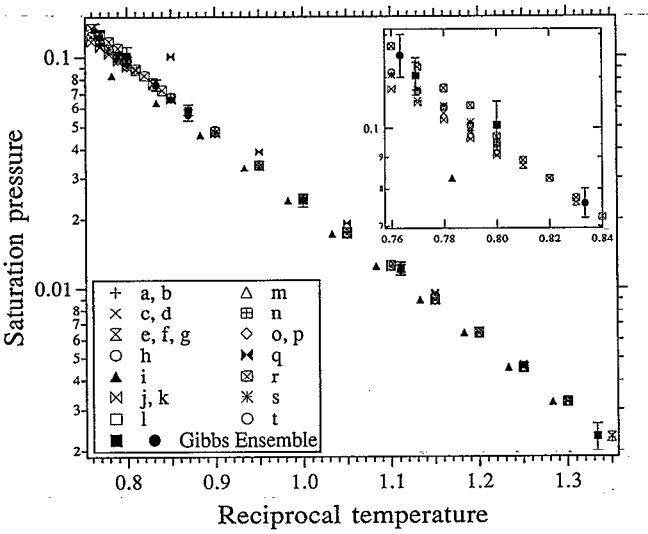


FIG. 7. Saturation pressure as a function of reciprocal temperature for the Lennard–Jones fluid. Letters in the legend indicate the Gibbs–Duhem series as defined in Table II; series with duplicate symbols do not overlap temperatures and thus can be distinguished by their location on the diagram. Filled markers represent Gibbs-ensemble data of Panagiotopoulos *et al.*[4] (squares) and of Smit *et al.*[17] (circles). The inset highlights the critical region.

Their absence suggests that the coupled sampling does not completely mimic the Gibbs ensemble as designed. A look at the Jacobian introduced with the coupling, Eq. (2.7), indicates that the densities are discouraged from sampling values close to the arbitrarily imposed "overall density" $\rho$. Thus a histogram of the system densities would likely not display the anomalous "third peak" at $\rho$ described by Smit *et al.*[5] and discounted by Mon and Binder.[19] While this difference seems to have had no adverse effect on the simulation averages, a more extensive investigation of the influence of the artificial coupling on the Gibbs–Duhem procedure would certainly be worthwhile.

The coexistence results of all studies are presented in Figs. 7 and 8. The data are on the whole consistent and reproducible, and the procedure seems largely insensitive to the details of its implementation. Agreement with the established coexistence data[4,17] is very good. Nevertheless several discrepancies are apparent. Approach to the critical is a topic in itself, and it receives extensive discussion below. In addition, two entire series differ conspicuously from the others: (1) that which uses low-temperature Gibbs ensemble data[4] for the initial condition, series (i); and (2) the "worst-case" implementation in which Eq. (1.2) is integrated using the trapezoid rule with a large step size, series (q). In the former, error introduced at an early stage propagates through the entire series, and it highlights the need for reliable initial-condition data. A temperature intermediate between the triple and critical points seems a good choice for the initial condition (if using the results of a Gibbs ensemble run as the source of the data). Starting from this condition, the Gibbs–Duhem method retraces its path with essentially no deviation when series are conducted to low temperatures and back again. The "worst-case" example shows that the method cannot be used carelessly even if good initial-condition data are available, and that the technique indeed has limits.

The anticipated failure of the Gibbs–Duhem method was observed in most series upon approach of the critical temperature. In the majority of instances, the series was terminated because the liquid phase took on vaporlike values. The inset of Fig. 7 reveals that in the critical region the Gibbs–Duhem pressures are lower than those given by the Gibbs ensemble simulations—the difference is slight but

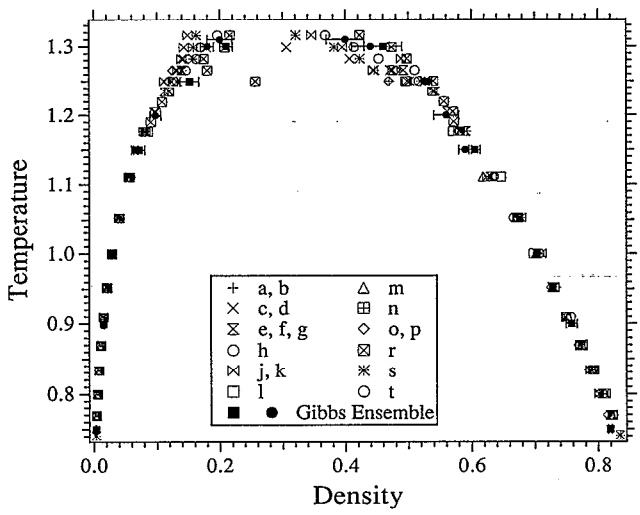


FIG. 8. Coexistence envelope of the Lennard-Jones fluid. Symbols are as in Fig. 7.

consistent. The discrepancy explains the poor reproducibility of the liquid-phase densities seen in Fig. 8, and the tendency of the liquid to vaporize. Introduction of the coupling method did indeed preclude this unilateral phase change, but the results still suffered greatly from the poor estimate of the pressure. Most of the high-temperature simulations that incorporated this technique are substantially in error, with liquid- and vapor-phase densities that are clearly too low near the critical. This behavior is consistent with that found in the study of the van der Waals model described in the previous section, in which any error in the pressure tended toward its underestimation.

The single most effective means for improving the results near the critical point was to decrease the step size of the Gibbs–Duhem integration. This measure greatly improved the pressure estimate and thereby eliminated the main cause of the scatter in the data of Fig. 8. Series (r), (s), and (t) each integrated with a step of 0.01 at high temperatures [series (d) and (j) also used this small step, but they were initiated with a poorly estimated pressure]. In each series the pressure was brought more in line with the Gibbs ensemble results. Moreover, the coupling technique of Sec. II C proved very successful in eliminating unilateral phase transitions while maintaining the integrity of the results. As with any simulation near a critical point, system size and sampling duration greatly influenced the outcome. Bad luck in the middle of series (r) resulted in a vapor density that is clearly too high, and this skewed the rest of the series (interestingly enough, to higher pressures). Series (s) began from the last "good" run of series (r). Using the same initial configuration and a different random number seed, it sampled 30 000 cycles with satisfactory results; even the first 10 000 cycles [the duration of the series (r) runs] of the first run of this series averaged to a reasonable density. Still, at temperatures very near the critical the results deteriorated, particularly the vapor density. The trouble was alleviated in series (t), where 256 particles simulated each phase and much better results were obtained at even the highest temperatures.

Figure 9 and Table III summarize the results from what should be the best series: those having 256 particles in each phase, the highest-order integration scheme, the best choice of governing equation, and the smallest step size for the region integrated. These are series (o) for the low temperatures and series (t) near the critical point; the 108 particle-per-phase simulations of series (r) are also included where they do not overlap these larger system simulations. The table shows that the pressure of each phase is consistent with the imposed pressure, and that the data satisfy the Gibbs–Duhem consistency test for the chemical potentials. A fit of the vapor pressure to the Antoine equation

$$\ln P^{\text{sat}} = A - \frac{B}{T+C} \tag{3.2}$$

yields the constants: $A=3.31885$; $B=7.31828$; $C=0.039433$. The figure highlights the ability of Gibbs–Duhem integration—when properly implemented—to provide accurate results over the entire range of temperature.

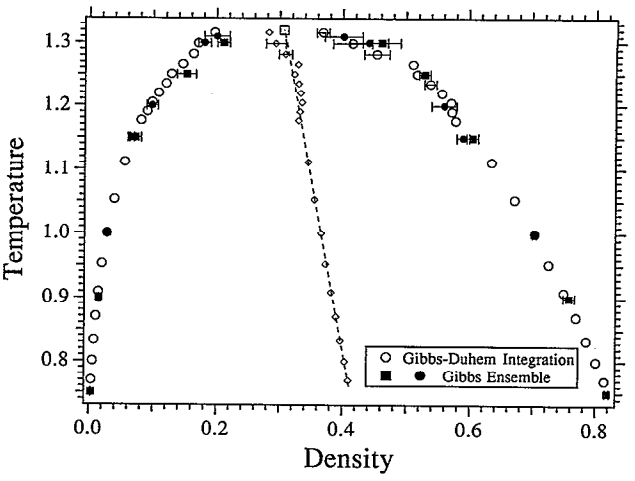


FIG. 9. Coexistence envelope of the Lennard-Jones fluid. Open circles represent the Gibbs–Duhem data of series (o), (r), and (t), and the filled markers represent Gibbs ensemble data of Panagiotopoulos *et al.*[4] (squares) and of Smit *et al.*[17] (circles). Error bars are included only if larger than the plot marker. The diamonds describe the law of rectilinear diameter, and the critical point estimated from the data is indicated by the square.

These data are all within the experimental error of the Gibbs ensemble results, although very near the critical point they still differ consistently and may yet benefit from a smaller integration step. Nevertheless, these data constitute the most extensive simulation results to date for the vapor–liquid coexistence properties of the Lennard-Jones fluid.

Following Smit,[17] the critical parameters may be estimated by an analysis of the approach to the critical. The critical temperature $T_c$ and density $\rho_c$ are obtained from a least-squares fit of the law of rectilinear diameter

$$\frac{\rho_l+\rho_v}{2} = \rho_c + C_1(T-T_c) \tag{3.3}$$

and the critical scaling relation

$$\rho_l - \rho_v = C_2(T_c-T)^{\beta_c}, \tag{3.4}$$

where $\rho_l$ and $\rho_v$ are the liquid and vapor densities, respectively, and $C_1$ and $C_2$ are fitting parameters. The critical exponent $\beta_c$ (written with the subscript to distinguish it from the reciprocal temperature) is taken as 0.32. Details of the analysis follow the thorough description given by Smit.[17] The fit of Eq. (3.3) was performed over the entire range of temperature, and the result is included in Fig. 9. Equation (3.4) was fit using only data for which $T>1.15$, and Fig. 10 shows how it describes the approach to the critical. The data indicate

$$T_c = 1.321 \pm 0.004,$$

$$\rho_c = 0.306 \pm 0.001.$$

These results are in complete agreement with the conclusions of Smit: $T_c=1.316\pm0.006$, $\rho_c=0.304\pm0.006$. Further, the analysis is not particularly sensitive to the location of the temperature cutoff for the fit of Eq. (3.4). Use

TABLE III. Simulation results from series (o), (r), and (t). All quantities are given in Lennard-Jones units. $\beta$ is the reciprocal temperature, $T$ is the temperature (provided for convenience), $P(p/c)$ is the final value of the pressure as estimated by the corrector formula. The next three column pairs report simulation averages for the pressure, molar density, and molar energy in each phase. The small subscripts indicate the accuracy of the last digit, so $5.85_1$ means $5.85\pm0.01$; this reflects only the statistical error of the simulations, and does not attempt to incorporate any systematic errors that might result from the predictor–corrector integration method. The quantity $\Delta(\beta\mu)$ is the change in chemical potential from its value at the initial condition $\beta=1.35$ [given by a series (e) simulation], and it is determined from the simulation data of each phase by applying simple trapezoid rule integration to the Gibbs–Duhem equation as written $d(\beta\mu)=h\,d\beta+\beta P/\rho\,d\ln P$, where the molar enthalpy $h=u+P/\rho$. Entries with no $\Delta(\beta\mu)$ values reported are not considered "best" results for the temperature and are provided only for comparison; these data are not presented in Fig. 9 and were not used to determine the critical properties.

| | | | $P$(sim) | | $\rho$ | | $-u$ | | $\Delta(\beta\mu)$ | |
|---|---|---|---|---|---|---|---|---|---|---|
| $\beta$ | $T$ | $P(p/c)$ | vapor | liquid | vapor | liquid | vapor | liquid | vapor | liquid |
| Series (o) | | | | | | | | | | |
| 1.35 | 0.741 | 0.00229 | $0.00225_1$ | $0.02_2$ | 0.00313 | 0.835 | 0.0360 | 6.02 | 0.0 | 0.0 |
| 1.30 | 0.769 | 0.00321 | $0.00316_2$ | $0.04_2$ | $0.00433_3$ | $0.815_1$ | $0.0487_7$ | $5.85_1$ | 0.296 | 0.298 |
| 1.25 | 0.800 | 0.00452 | $0.00445_5$ | $0.01_3$ | $0.00591_4$ | $0.801_2$ | $0.064_1$ | $5.73_1$ | 0.589 | 0.589 |
| 1.20 | 0.833 | 0.00633 | $0.00627_5$ | $0.02_3$ | $0.00807_6$ | $0.786_1$ | $0.086_2$ | $5.60_1$ | 0.874 | 0.875 |
| 1.15 | 0.870 | 0.00886 | $0.00877_8$ | $0.00_3$ | $0.01101_7$ | $0.769_1$ | $0.113_2$ | $5.46_1$ | 1.152 | 1.154 |
| 1.10 | 0.909 | 0.0124 | $0.0124_1$ | $-0.00_2$ | $0.0151_1$ | $0.750_2$ | $0.151_2$ | $5.29_1$ | 1.425 | 1.428 |
| 1.05 | 0.952 | 0.0173 | $0.0174_2$ | $-0.01_3$ | $0.0207_2$ | $0.726_1$ | $0.200_3$ | $5.09_1$ | 1.691 | 1.694 |
| 1.00 | 1.000 | 0.0242 | $0.0246_2$ | $0.04_3$ | $0.0284_2$ | $0.704_2$ | $0.265_3$ | $4.92_2$ | 1.949 | 1.952 |
| 0.95 | 1.053 | 0.0338 | $0.0343_4$ | $0.02_2$ | $0.0395_3$ | $0.672_2$ | $0.360_4$ | $4.66_1$ | 2.200 | 2.203 |
| 0.90 | 1.111 | 0.0471 | $0.0475_6$ | $0.06_2$ | $0.0557_4$ | $0.635_3$ | $0.488_5$ | $4.39_2$ | 2.441 | 2.446 |
| 0.85 | 1.176 | 0.0659 | $0.0655_8$ | $0.07_3$ | $0.0810_8$ | $0.578_4$ | $0.689_9$ | $3.97_3$ | 2.672 | 2.677 |
| 0.80 | 1.250 | 0.0911 | $0.093_2$ | $0.09_1$ | $0.118_2$ | $0.47_3$ | $0.95_1$ | $3.2_2$ | ··· | ··· |
| Series (r) | | | | | | | | | | |
| 0.84 | 1.190 | 0.0723 | $0.069_2$ | $0.06_3$ | $0.091_2$ | $0.572_7$ | $0.76_1$ | $3.91_4$ | 2.717 | 2.722 |
| 0.83 | 1.205 | 0.0774 | $0.077_2$ | $0.12_3$ | $0.098_1$ | $0.571_7$ | $0.81_1$ | $3.90_5$ | 2.762 | 2.767 |
| 0.82 | 1.220 | 0.0830 | $0.081_2$ | $0.14_3$ | $0.108_2$ | $0.556_6$ | $0.88_2$ | $3.80_4$ | 2.807 | 2.813 |
| 0.81 | 1.235 | 0.0889 | $0.088_3$ | $0.12_3$ | $0.120_4$ | $0.538_9$ | $0.96_3$ | $3.67_6$ | 2.851 | 2.857 |
| 0.80 | 1.250 | 0.0970 | $0.093_{10}$ | $0.12_3$ | $0.26_2$ | $0.540_8$ | $1.91_9$ | $3.67_5$ | ··· | ··· |
| Series (t) | | | | | | | | | | |
| 0.80 | 1.250 | 0.0952 | $0.096_2$ | $0.10_1$ | $0.128_2$ | $0.517_7$ | $1.04_2$ | $3.54_5$ | 2.894 | 2.901 |
| 0.79 | 1.266 | 0.1020 | $0.102_3$ | $0.09_2$ | $0.146_4$ | $0.510_7$ | $1.16_3$ | $3.49_4$ | 2.938 | 2.945 |
| 0.78 | 1.282 | 0.1094 | $0.109_3$ | $0.11_1$ | $0.163_4$ | $0.45_2$ | $1.29_3$ | $3.1_1$ | 2.981 | 2.987 |
| 0.77 | 1.299 | 0.1167 | $0.120_3$ | $0.13_1$ | $0.170_4$ | $0.41_3$ | $1.33_3$ | $2.9_2$ | 3.021 | 3.028 |
| 0.76 | 1.316 | 0.1240 | $0.132_4$ | $0.14_1$ | $0.196_7$ | $0.37_1$ | $1.51_5$ | $2.59_6$ | 3.060 | 3.067 |

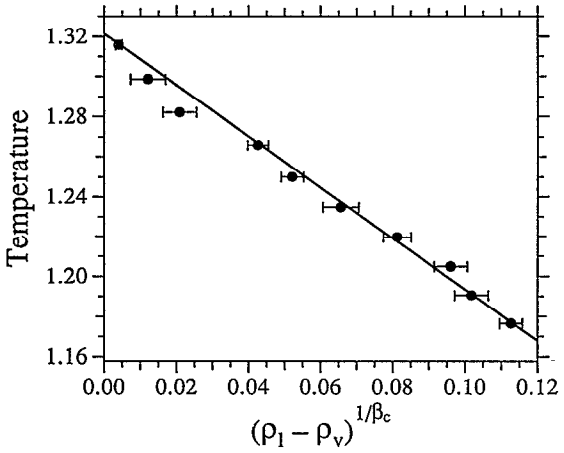


FIG. 10. The critical scaling relation of Eq. (3.3) formulated to permit linear least-squares analysis. $\rho_l$ and $\rho_v$ are the liquid and vapor densities, respectively, and the critical exponent $\beta_c$ is taken as 0.32. Solid line is the resulting best fit to the data.

of only the data for which $T>1.28$ (the last three coexistence points) yields $T_c=1.324\pm0.012$, $\rho_c=0.305\pm0.002$. Of course a proper determination of the critical point in the thermodynamic limit requires a study of system size;[19] the excellent agreement between our results and Smit's merely demonstrates that the Gibbs–Duhem technique provides correct results for a given finite system.

## IV. DISCUSSION

### A. Assessment

The most important feature of the Gibbs–Duhem technique is obvious: It provides for the accurate, robust, and efficient evaluation of phase equilibria by molecular simulation. Each coexistence point is determined by a single simulation, and there is no need for particle exchanges to enforce chemical potential equality. It is the only simulation technique that offers this combination of features. Challenging phase equilibria calculations may be approached—and in some cases for the first time—with this technique. However, the method is not without its drawbacks, and at the same time it has other advantages of lesser importance; these issues warrant discussion.

The ability of the method to handle all types of weakly first-order phase transitions is not yet demonstrated. Two distinct concerns arise: First, the free energy barrier separating coexisting phases of this type is sometimes small; second, the difference in the thermodynamic properties of these phases is (by definition) also small. The first issue is less serious. A small free energy barrier may lead to difficulty in preventing each simulation volume from sampling both coexisting regions. Usually this occurs near a critical point, as seen in the case of the Lennard-Jones simulation above. However, a weakly first-order transition is not necessarily accompanied by a low free-energy barrier, and in such instances the simulation may be conducted without concern that the subsystems will freely sample both phases. When it does arise, the problem is one of too much rather than not enough sampling, and finding ways to limit sampling is not an inherently difficult problem. Appropriate steps—such as the coupling technique successfully used above—can be developed to overcome this complication. The second difficulty of weak first-order transitions is of greater concern. To propagate along the saturation line, the Gibbs–Duhem method requires accurate evaluation of differences between the two coexisting phases. If these differences are too small, it may prove difficult to evaluate them with sufficient accuracy—the statistical error for each phase could well be greater than the difference between the phases. The extent to which this happens will depend on the thermodynamic properties to be evaluated. In all instances the required properties are first derivatives of the free energy, which are typically well determined by simulations of reasonable size and duration. In the examples discussed in this report, the enthalpy and the volume are needed; these are among the most reliable and easily evaluated quantities that may be determined by simulation. Still, in situations where the small difference is a problem the only apparent solution is additional sampling. The degree to which Gibbs–Duhem integration scheme is sensitive to statistical errors in these instances is an open question that must be addressed.

The Gibbs–Duhem integration method relies on accurate initial-condition data. As demonstrated in the applications above, errors in these data will propagate, and can invalidate the entire series. This is not an issue with Gibbs ensemble simulation, where each coexistence measurement is independent. Furthermore, other unforeseen errors may accrue in a Gibbs–Duhem series, and one of the problems with the method is that it is difficult to determine if any such errors are present; with the Gibbs ensemble one may compute the chemical potential and pressure of each phase and determine if they agree. A particularly effective means for verifying the results of a Gibbs–Duhem series is to check it against a "final condition"—coexistence data obtained independently for the series endpoint. The VLE studies described above do not lend themselves naturally to such a comparison, but other studies could. Mixtures are an obvious example—one may conduct a series for a binary mixture beginning from pure component $A$ to pure component $B$. The check is easily performed if the coexistence properties of the pure substances are known. Such a check is not required for application of the Gibbs–Duhem technique, but when possible it should be done.

Gibbs–Duhem may be implemented using molecular dynamics. While we have not attempted such a calculation, NPT MD is now a standard procedure[1] and there is no indication that it could not be used as the basis of a Gibbs–Duhem program. Molecular dynamics is of course essential if one wishes to examine any temporally based quantities, such as the transport coefficients. Also, for some potentials MD samples configurations much more efficiently than does MC. An MD-based implementation of Gibbs ensemble simulation would be difficult to implement, although it is not out of the question.

One of the appealing features of Panagiotopoulos' Gibbs ensemble technique is its simplicity. In its basic form it is little more difficult to program than a grand-canonical simulation. This important feature is not lost with Gibbs–Duhem method, and in fact it may be argued that Gibbs–Duhem simulation is in some ways simpler to conduct. The absence of particle exchange between the phases eliminates the bookkeeping needed to monitor the positions of a variable number of particles in each simulation volume. This consideration makes efficient implementation of the Gibbs ensemble algorithm troublesome, particularly if one wishes to exploit the features of multiple-processor computers. Moreover, the need for exchange steps in a Gibbs ensemble simulation means that the number of particles used to model each phase is unknown at the outset of the run. One must be careful that an adequate number remain in each phase. These "technical" challenges accompanying particle interchange are not a concern in a Gibbs–Duhem simulation. On the other hand, in a Gibbs–Duhem simulation proper implementation of the predictor–corrector formulas requires coordination of the results of several simulations; this is especially troublesome if one wishes more freedom in choosing the state conditions than is afforded by the constant-step size formulas presented in Table I.

It is quite natural to compare the Gibbs–Duhem technique to the Gibbs ensemble method, and indeed such a comparison has arisen several times in the discussion above. Still, the two methods should be viewed as complementary rather than competing approaches to the problem of coexistence evaluation in model systems. There are many difficult problems to which the Gibbs ensemble cannot be applied, and to which Gibbs–Duhem integration may. On the other hand, Gibbs–Duhem is not appropriate for evaluation of coexistence of a single or even a few random state points; its strength is the mapping of entire phase diagrams. And of course Gibbs–Duhem integration requires startup data, the "initial condition." The Gibbs ensemble is the method of choice for supplying this information. In sum, the Gibbs–Duhem technique for evaluation of phase coexistence offers many features, but much of its value remains to be proved. Before concluding, we should briefly discuss some extension of the technique.

### B. Extensions

Many interesting "extensions" of the Gibbs–Duhem method outlined above are really just direct application of

the same equations to other coexistence phenomena: freezing, liquid–crystal transitions, liquid–liquid equilibria, etc. Often the quantity of interest is again the saturation pressure as a function of temperature, and no modification of the method is needed from that outlined above. Other less obvious extensions are possible, and we offer a few examples below.

Perhaps the most important extension of the proposed method is to mixtures. In a typical situation one would like to evaluate vapor–liquid coexistence compositions of a binary mixture as a function of temperature for a fixed pressure. The governing differential equation may be written

$$\left(\frac{\partial\beta}{\partial\xi}\right)_{p,\sigma}=\frac{x-y}{\Delta h\,\xi(1-\xi)}, \tag{4.1}$$

where $\Delta h=h_l-h_v$ is the difference between the liquid and vapor molar enthalpies, $x$ and $y$ are the liquid and vapor mole fractions, respectively, and $\xi$ is the so-called fugacity fraction.[20] Each simulation in this series is conducted in a semigrand ensemble,[21] which means it is performed at constant temperature, pressure, fugacity fraction, and total mole number; the species identity of each molecule—much like its spatial coordinates—changes during the simulation, with the imposed fugacity fraction governing the acceptance of each proposed change. The insertion problem begins to resurface in this approach, but to a much lesser extent; if the species are very unlike each other, acceptance of identity changes will be rare and the composition will not converge correctly. Startup of the Gibbs–Duhem series most naturally uses the pure fluid as the initial condition. The integrand is ill-defined in this limit, but it may be determined given the Henry's constant of the dilute component in the other.[20] Modification to include additional components is simple, but in doing so the number of interesting thermodynamic pathways increases greatly and it becomes difficult to give here a general prescription for the technique.

An appealing feature of the application of thermodynamic integration via molecular simulation is the ability to construct artificial paths of integration.[22] One may evaluate changes in thermodynamic properties as one potential evolves into another. The idea is easily carried over to the Gibbs–Duhem technique. The governing differential equation will likely be given in terms of atypical thermodynamic quantities, but they may in general be readily evaluated in each phase during the simulation and the Gibbs–Duhem integration algorithm may be applied without modification. As an example one could evaluate solid–fluid coexistence in anisotropic substances as a function of the molecular aspect ratio $\alpha$. If for example freezing of hard ellipsoids is to be investigated, one would begin with an aspect ratio of unity (hard spheres) using the result of Hoover and Ree.[23] The quantity to be averaged is the change in Gibbs free energy (the free enthalpy) with aspect ratio, $\lambda=(\partial\beta G/\partial\alpha)_{\beta P}$. In a simulation $\lambda$ can be determined from the fraction of the configurations that result in overlap when $\alpha$ is increased or decreased by some small amount. The equation to be integrated by the Gibbs–Duhem series is

$$\left(\frac{\partial\beta P}{\partial\alpha}\right)_{\beta,\sigma}=\frac{\Delta\lambda}{\Delta v}, \tag{4.2}$$

where $\Delta$ indicates the difference between the coexisting phases ($v$, as above, is the molar volume). One may integrate along the direction of increasing $\alpha$ (prolate) or decreasing $\alpha$ (oblate). This calculation would provide a good test of the versatility of the Gibbs–Duhem technique. Freezing is a much weaker transition than condensation (examined in the test studies above), and $\lambda$ is not likely to be evaluated as accurately as the internal energy.

With the advent of the Gibbs ensemble it became possible to evaluate phase coexistence with a single simulation. The Gibbs–Duhem method suggests a way of taking this advance one step further: *the entire coexistence envelope* determined from a single simulation. Using vapor–liquid coexistence again as the example, one might achieve this feat with a Gibbs–Duhem series by gradually increasing the temperature in small amounts during the entire simulation. One might conduct a simulation lasting, say, 50 000 cycles, where at the end of each cycle the temperature is incremented by 0.00 002 units. At all times the system is differentially removed from equilibrium, and a truly reversible path is negotiated from the triple point to the critical point. Compared to the discrete integration method described above (e.g., five 10 000-cycle simulations each at a fixed temperature), this single-simulation approach has the certain advantages of a very small error of integration (due to the very small integration step size) and the elimination of "wasted" equilibration steps. Evaluation of the feasibility and efficiency of a single-simulation phase diagram calculation would require a separate study. No doubt the concept on its face is appealing.

## ACKNOWLEDGMENTS

Financial support for this work has been provided by the National Science Foundation, under grant CTS-8909365 and under the Presidential Young Investigator program. The author is grateful to the reviewer of the manuscript for bringing Ref. 2 to his attention.

[1] M. P. Allen and D. J. Tildesley, *Computer Simulation of Liquids* (Clarendon, Oxford, 1987).
[2] A. D. Bruce and N. B. Wilding, Phys. Rev. Lett. **68**, 193 (1992); N. B. Wilding and A. D. Bruce, J. Phys.: Condens. Matter **4**, 3087 (1992).
[3] A. Z. Panagiotopoulos, Mol. Phys. **61**, 813 (1987).
[4] A. Z. Panagiotopoulos, N. Quirke, M. Stapleton, and D. J. Tildesley, Mol. Phys. **63**, 527 (1988).
[5] B. Smit, P. de Smedt, and D. Frenkel, Mol. Phys. **68**, 931 (1989).
[6] A. Z. Panagiotopoulos, Mol. Sim. **9**, 1 (1992).
[7] M. Laso, J. J. de Pablo, and U. W. Suter, J. Chem. Phys. **97**, 2817 (1992).
[8] G. C. A. M. Mooij, D. Frenkel, and B. Smit, J. Phys.: Condens. Matter **4**, L255 (1992).
[9] D. A. Kofke, Molec. Phys. (in press).
[10] K. Denbigh, *Principles of Chemical Equilibrium* (Cambridge University, Cambridge, 1971).
[11] C. W. Gear, *Numerical Initial Value Problems in Ordinary Differential Equations* (Prentice-Hall, Englewood Cliffs, NJ, 1971).
[12] B. A. Finlayson, *Nonlinear Analysis in Chemical Engineering* (McGraw-Hill, New York, 1980).
[13] B. Carnahan, H. A. Luther, and J. O. Wilkes, *Applied Numerical Methods* (Wiley, New York, 1969).

[14] W. H. Press, B. P. Flannery, S. A. Teukolsky, and W. T. Vetterling, *Numerical Recipes: The Art of Scientific Computing* (Cambridge University, Cambridge, 1988).
[15] H. B. Callen, *Thermodynamics and an Introduction to Thermostatistics* (Wiley, New York, 1985).
[16] D. A. McQuarrie, *Statistical Mechanics* (Harper & Row, New York, 1976).
[17] B. Smit, Ph.D. thesis, University of Utrecht, The Netherlands (1990).
[18] J. Kolafa, Molec. Phys. **59**, 1035 (1986).
[19] K. K. Mon and K. Binder, J. Chem. Phys. **96**, 6989 (1992).
[20] D. A. Kofke and E. D. Glandt, Molec. Phys. **64**, 1105 (1988).
[21] J. G. Briano and E. D. Glandt, J. Chem. Phys. **80**, 3336 (1984).
[22] D. Frenkel, in *Proceedings of the NATO ASI on Computer Modeling of Fluids, Polymers and Solids*, edited by C. R. A. Catlow (Kluwer Academic, Dordrecht, The Netherlands, 1989).
[23] W. G. Hoover and F. H. Ree, J. Chem. Phys. **49**, 3609 (1968).